

Phase transition behaviors in relaxor  
ferroelectric [001]-poled  
Pb(In<sub>1/2</sub>Nb<sub>1/2</sub>)O<sub>3</sub>-Pb(Mg<sub>1/3</sub>Nb<sub>2/3</sub>)O<sub>3</sub>-PbTiO<sub>3</sub>  
single crystals studied by Brillouin light  
scattering and dielectric spectroscopies

著者	Kim Tae Hyun, Kojima Seiji, Ko Jae-Hyeon
journal or publication title	Journal of applied physics
volume	111
number	5
page range	054103
year	2012
権利	Copyright (2012) American Institute of Physics. This article may be downloaded for personal use only. Any other use requires prior permission of the author and the American Institute of Physics. The following article appeared in J. Appl. Phys. 111, 054103 (2012) and may be found at <a href="http://jap.aip.org/resource/1/japiau/v111/i5/p054103_s1?ver=pdfcov">http://jap.aip.org/resource/1/japiau/v111/i5/p 054103_s1?ver=pdfcov</a> .
URL	<a href="http://hdl.handle.net/2241/117000">http://hdl.handle.net/2241/117000</a>

## Phase transition behaviors in relaxor ferroelectric [001]-poled $\text{Pb}(\text{In}_{1/2}\text{Nb}_{1/2})\text{O}_3\text{-Pb}(\text{Mg}_{1/3}\text{Nb}_{2/3})\text{O}_3\text{-PbTiO}_3$ single crystals studied by Brillouin light scattering and dielectric spectroscopies

Tae Hyun Kim, Seiji Kojima, and Jae-Hyeon Ko

Citation: *J. Appl. Phys.* 111, 054103 (2012); doi: 10.1063/1.3692596

View online: <http://dx.doi.org/10.1063/1.3692596>

View Table of Contents: <http://jap.aip.org/resource/1/JAPIAU/v111/i5>

Published by the American Institute of Physics.

### Related Articles

Defect chemistry of Ti-doped antiferroelectric  $\text{Bi}_{0.85}\text{Nd}_{0.15}\text{FeO}_3$   
*Appl. Phys. Lett.* 100, 182902 (2012)

Density functional investigations on electronic structures, magnetic ordering and ferroelectric phase transition in multiferroic  $\text{Bi}_2\text{NiMnO}_6$   
*AIP Advances* 2, 022115 (2012)

Structural phase transitions in Ti-doped  $\text{Bi}_{1-x}\text{Nd}_x\text{FeO}_3$  ceramics  
*J. Appl. Phys.* 111, 064107 (2012)

Thickness driven stabilization of saw-tooth-like domains upon phase transitions in ferroelectric thin films with depletion charges  
*J. Appl. Phys.* 111, 064105 (2012)

Magnetic enhancement across a ferroelectric-antiferroelectric phase boundary in  $\text{Bi}_{1-x}\text{Nd}_x\text{FeO}_3$   
*J. Appl. Phys.* 111, 053927 (2012)

### Additional information on J. Appl. Phys.

Journal Homepage: <http://jap.aip.org/>

Journal Information: [http://jap.aip.org/about/about\\_the\\_journal](http://jap.aip.org/about/about_the_journal)

Top downloads: [http://jap.aip.org/features/most\\_downloaded](http://jap.aip.org/features/most_downloaded)

Information for Authors: <http://jap.aip.org/authors>

### ADVERTISEMENT

**IBD Optical Film Quality at PVD Rates**

Advanced Optical Thin Films

Wide Range of Applications

Superior Throughput and Repeatability

**SPECTOR-HT ION BEAM DEPOSITION SYSTEMS**

**Veeco**  
Innovation. Performance. Brilliant.

[www.veeco.com/spectorht](http://www.veeco.com/spectorht)

# Phase transition behaviors in relaxor ferroelectric [001]-poled $\text{Pb}(\text{In}_{1/2}\text{Nb}_{1/2})\text{O}_3\text{-Pb}(\text{Mg}_{1/3}\text{Nb}_{2/3})\text{O}_3\text{-PbTiO}_3$ single crystals studied by Brillouin light scattering and dielectric spectroscopies

Tae Hyun Kim,<sup>1</sup> Seiji Kojima,<sup>1,a)</sup> and Jae-Hyeon Ko<sup>2,b)</sup><sup>1</sup>Graduate School of Pure and Applied Sciences, University of Tsukuba, Tsukuba city, Ibaraki 305-8573, Japan<sup>2</sup>Department of Physics, Hallym University, 39 Hallymdaehakgil, Chuncheon, Gangwondo 200-702, South Korea

(Received 27 January 2012; accepted 11 February 2012; published online 8 March 2012)

Phase transition behaviors of [001]-oriented  $\text{Pb}(\text{In}_{1/2}\text{Nb}_{1/2})\text{O}_3\text{-Pb}(\text{Mg}_{1/3}\text{Nb}_{2/3})\text{O}_3\text{-PbTiO}_3$  (PIN-PMN-PT) single crystals were studied under unpoled and [001]-poled conditions by Brillouin light scattering and dielectric spectroscopies. The unpoled crystal showed a diffused elastic anomaly accompanied by substantial dielectric dispersion, which were associated with the temperature evolution of polar nanoregions represented by the excitation of strong central peaks. The poled crystal exhibited two-step changes in both dielectric and elastic properties, which were attributed to the successive phase transitions from rhombohedral to tetragonal, and then from tetragonal to cubic phase upon heating. The high-temperature tetragonal-cubic phase transition remained diffused with dielectric dispersion due to local random fields inherent in relaxors. The transverse acoustic mode disappeared at the rhombohedral-tetragonal phase transition indicating a clear symmetry change. © 2012 American Institute of Physics. [<http://dx.doi.org/10.1063/1.3692596>]

## I. INTRODUCTION

Lead-based complex perovskite single crystals such as  $\text{Pb}[(\text{Zn}_{1/3}\text{Nb}_{2/3})_{1-x}\text{Ti}_x]\text{O}_3$  (PZN-*x*PT) and  $\text{Pb}[(\text{Mg}_{1/3}\text{Nb}_{2/3})_{1-x}\text{Ti}_x]\text{O}_3$  (PMN-*x*PT) have been studied intensively due to their excellent piezoelectric performances since the pioneering work by Park *et al.*<sup>1</sup> The piezoelectric coefficient  $d_{33}$  and the electromechanical coupling constant  $k_{33}$  of these systems were shown to be more than 2000 pC/N and 90% when the composition *x* was located near the morphotropic phase boundary (MPB). However, PZN-*x*PT and PMN-*x*PT suffer from several drawbacks, i.e., low Curie temperature ( $T_c$ ), low R-T (rhombohedral to tetragonal) transition temperature ( $T_{RT}$ ), and low coercive field, all of these limiting the temperature and electric field usage ranges for practical applications. Extensive efforts have been focused on the improvement of thermal stability of these lead-based perovskite relaxor ferroelectrics by looking for new binary or ternary systems.<sup>2,3</sup>

Recently,  $\text{Pb}(\text{In}_{1/2}\text{Nb}_{1/2})\text{O}_3\text{-Pb}(\text{Mg}_{1/3}\text{Nb}_{2/3})\text{O}_3\text{-PbTiO}_3$  (PIN-PMN-PT) ternary system was found to show higher phase transition temperatures along with comparable piezoelectric performances to PMN-*x*PT,<sup>4-8</sup> which is expected to broaden the temperature and electric field ranges for applications as piezoelectric devices. Recently, various properties of PIN-PMN-PT single crystals near MPB including elastic, dielectric, and piezoelectric properties have been studied under different poling conditions.<sup>9-21</sup> However, the ferroelectric phase transition behaviors of PIN-PMN-PT single crystals have not been studied in detail. A great portion of the published data on this system are reported on poled samples at room temperatures, and studies on the phase transition behav-

iors in the temperature window of as-grown or unpoled samples in comparison with poled ones are scarce. The dielectric constant at the Curie temperature of PZN-*x*PT and PMN-*x*PT near MPB usually exhibits very sharp, discontinuous changes while that of PIN-PMN-PT is broad and diffused.<sup>8</sup> These distinctive results suggest that the phase transition behaviors might be different between binary and ternary systems. Understanding of the phase transition behaviors under various conditions including dc bias field effect is prerequisite to improving material performances and practical applications of PIN-PMN-PT, which is the motivation of this study. We report on the temperature dependence of acoustic anomalies, quasielastic central peaks and dielectric properties of [001]-oriented PIN-PMN-PT single crystals under unpoled and poled conditions. The observed acoustic anomalies and excitation of central peaks will be discussed in detail in relation with the phase transition behaviors and dynamics of polar nanoregions (PNRs), which is one of the key concepts in the physics of relaxor ferroelectrics.

## II. EXPERIMENT

The single crystal used in the current study was supplied by TRS Technologies Inc. It was grown by the modified Bridgman method and has the nominal composition of 0.26PIN-0.46PMN-0.28PT. It is well known that the exact contents of PIN, PMN and PT vary along the growth direction and that the room-temperature symmetry and electromechanical properties depend on the sample position in the grown crystal.<sup>8,19</sup> The  $d_{33}$ ,  $k_{33}$  and free dielectric constant of [001]-poled crystals were 1340–1410 pC/N, 90–91%, and ~4310, respectively, at room temperature. These results indicate that the investigated crystals may be close to the part B of Ref. 8 and to the *R*(1) or *R*(2) single crystals of

<sup>a)</sup>Electronic mail: kojima@bkukuba.ac.jp.<sup>b)</sup>Electronic mail: hwangko@hallym.ac.kr. FAX: 82-33-256-3421.

Ref. 19. The crystal dimensions were  $5 \times 5 \times 0.5 \text{ mm}^3$ , and the largest surfaces were (001) pseudocubic planes. The Brillouin spectrum was measured in the backward scattering geometry by using a conventional tandem Fabry-Perot interferometer combined by a photomultiplier tube and a photon counting system. Gold was vacuum-sputtered to form electrodes on the largest (001) surfaces. The crystal was inserted in a silicon oil at room temperature and was poled along the  $[001]_c$  direction under a dc bias field of  $15 \text{ kV/cm}$  at  $30^\circ\text{C}$  for 1 h, where the subscript “c” represents cubic coordinates. After poling, the electrodes were removed and the Brillouin spectra were measured during the heating process. The wavelength of the excitation source was  $532 \text{ nm}$ . The polarization direction of the incident laser beam was in the (001) plane, which was perpendicular to the poling direction. There was no analyzer for the scattered beam during the measurement except when it was necessary to compare the polarized and depolarized components of central peaks. Either an LCR meter (3522-50, Hioki) or the Solartron impedance analyzer (SI1260) was used to measure the dielectric permittivity upon heating.

### III. RESULT AND DISCUSSION

Figure 1(a) shows three Brillouin spectra of unpoled PIN-PMN-PT at selected temperatures in a semi-log plot to put stress on the substantial changes in spectral features in a wide frequency and temperature ranges. Each spectrum consists of one Brillouin doublet corresponding to the longitudinal acoustic (LA) phonons and a central peak (CP). The absence of the transverse acoustic (TA) mode in the spectrum suggests that the average crystal symmetry is close to cubic even at low temperatures.<sup>22</sup> It is noticed that the LA mode frequency becomes softened and the CP intensity increases remarkably upon cooling. The polarized component of CP was much stronger than the depolarized component. The Brillouin spectrum was fitted by using response functions of the damped harmonic oscillator for the phonon modes and of the single Debye relaxator for CP, from which the Brillouin frequency shift ( $\nu_B$ ) of the acoustic phonons and the full-width at half-maximum (FWHM,  $\Gamma_B$ ) of phonons and CP were obtained. The inset of Fig. 1(a) shows the temperature dependence of the FWHM of CP, which is equal to  $1/\pi\tau$ , where  $\tau$  is the relaxation time of the relevant process responsible for CP. The temperature dependencies of  $\nu_B$  and  $\Gamma_B$  measured upon cooling and heating are shown in Figs. 2(a) and 2(b), respectively, for the unpoled PIN-PMN-PT single crystal. The real part of the complex dielectric constant ( $\epsilon'$ ) is also shown in Fig. 2(a) for comparison.  $\epsilon'$  shows maxima near  $200^\circ\text{C}$  of which the value is more than 40000 at 10 Hz. It exhibits frequency dispersion typical in relaxors, i.e., the dielectric maximum shifts to higher temperature with probe frequency. The temperature dependence of the characteristic relaxation frequency could be obtained from the dielectric maximum temperature  $T_m$  along with its probe frequency  $f$ , which were fitted by using the Vogel-Fulcher law  $f = f_0 \exp[-E/k_B(T_m - T_{VF})]$  where  $f_0$  is the attempted frequency,  $E$  the activation energy,  $k_B$  the Boltzmann constant, and  $T_{VF}$  the Vogel-Fulcher temperature. The best-fitted results are shown in the inset of Fig. 2(b) with

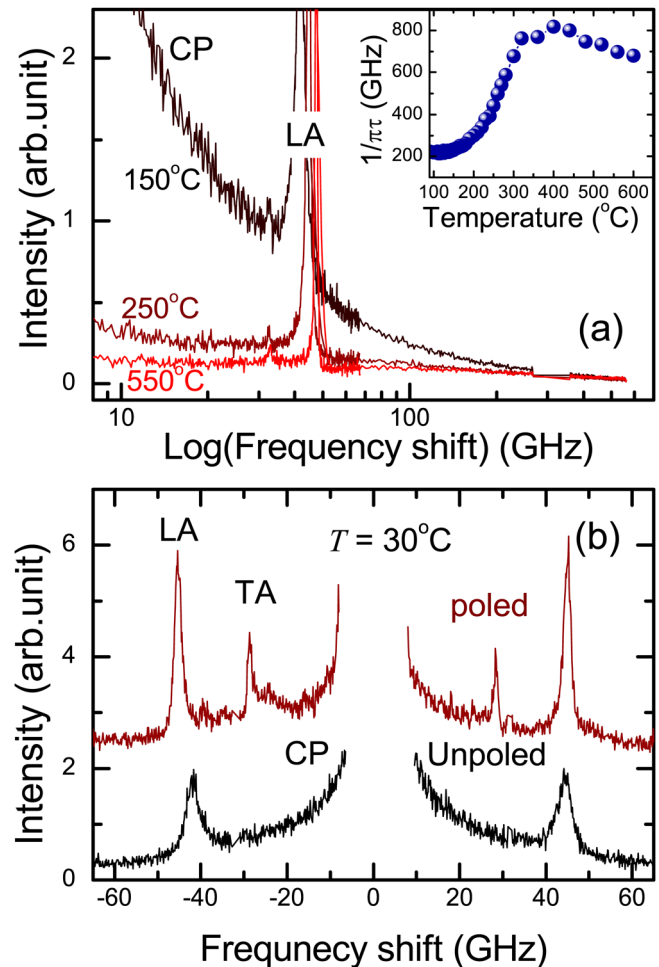


FIG. 1. (Color online) (a) The Brillouin spectra of  $[001]_c$ -oriented unpoled PIN-PMN-PT single crystals at a few temperatures in a wide frequency range. (b) The Brillouin spectra of unpoled and poled single crystal measured at  $30^\circ\text{C}$ . The inset of (a) shows the temperature dependence of FWHM of CP which is inversely proportional to the relaxation time  $\tau$ .

parameters  $f_0 = 4.6 \times 10^{12} \text{ Hz}$ ,  $E/k_B = 610 \text{ K}$ , and  $T_{VF} = 454 \text{ K}$  ( $= 182^\circ\text{C}$ ). These values of  $f_0$  and  $E/k_B$  are typical for relaxors.

Broad and frequency-dependent dielectric constants are correlated with the acoustic anomalies occurring in a wide temperature range.  $\nu_B$  shows almost a constant value at high temperatures from  $400^\circ$  to  $600^\circ\text{C}$ .  $\nu_B$  shows a substantial softening below  $\sim 300^\circ\text{C}$  accompanied by a significant increase in the hypersonic damping. These acoustic anomalies can be explained by the formation of PNRs and their electrostrictive coupling to the acoustic waves. As Fig. 1(a) shows, the growth of CP suggests the existence of polarization fluctuations. The most probable origin of these polarization fluctuations is the formation of PNRs at the so-called Burns temperature, although the microscopic origin of PNRs is still not settled completely.<sup>23</sup> The inset of Fig. 1(a) indicates a sudden change in  $\tau$  at about  $320^\circ\text{C}$ , below which the relaxation time rapidly increases and both  $\nu_B$  and  $\Gamma_B$  exhibit significant changes. This characteristic temperature may thus be assigned as the Burns temperature for the present PIN-PMN-PT single crystal at which PNRs begin to form. This Burns temperature is similar to that of PMN- $x$ PT ( $\sim 620 \text{ K} = 347^\circ\text{C}$ ).



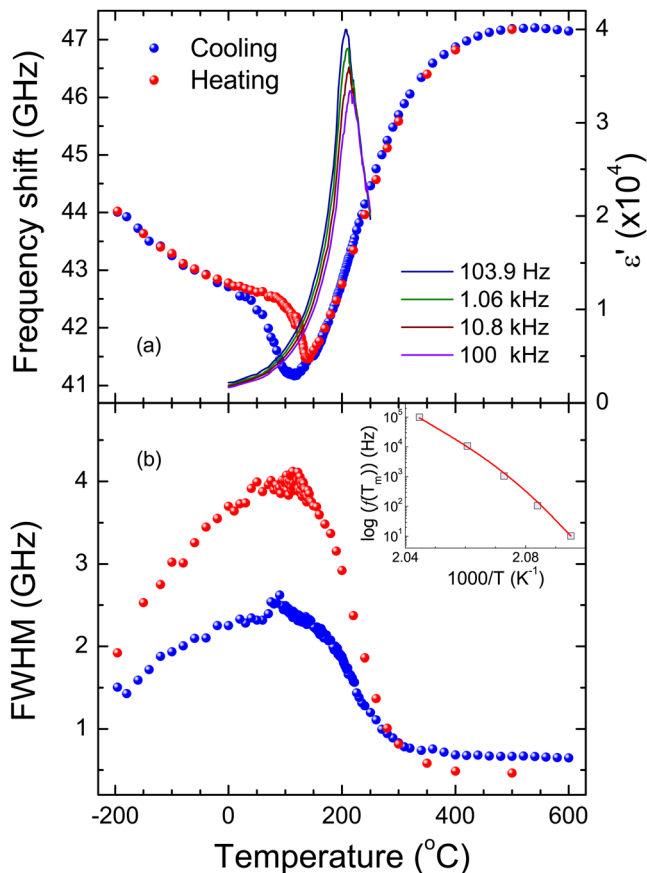


FIG. 2. (Color online) The temperature dependencies of (a) the Brillouin frequency shift and (b) the FWHM of the LA mode of the unpoled sample measured on both cooling and heating processes. The dielectric permittivity is shown in (a) for comparison. The inset of (b) is the characteristic relaxation frequency as explained in the text in the Arrhenius plot.

The increase in size and interactions between PNRs leads to the slowing down of their dynamics, which is reflected in both the increase in the relaxation time of CP [see the inset of Fig. 1(a)] and the diverging characteristic of the dielectric relaxation time represented by the Vogel-Fulcher behavior.  $\nu_B$  shows a minimum near 100 °C, and  $\Gamma_B$  displays a maximum at  $\sim 90$  °C, which may be attributed to the moderately diffused transformation into short-range (or mesoscopic) polar states. This transition may be attributed to some kinetic effect, i.e., the abrupt growth of PNRs at the (diffused) ferroelectric phase transition without changing the directions of their dipole moments due to the frustrated interactions between PNRs.<sup>24</sup> The correlation length of the polar domains would be very small and the average symmetry may not deviate from the prototype cubic phase appreciably, because TA mode, which is forbidden at the backward scattering geometry in the cubic phase, is not observed at low temperatures. Typical relaxor behaviors shown from both dielectric and elastic anomalies are also consistent with the observation of the labyrinthine domain pattern,<sup>17</sup> which is typical in relaxors, confirmed from similar compositions. Large thermal hysteresis can be noticed from both  $\nu_B$  and  $\Gamma_B$ , similar to PZN-4.5%PT.<sup>25</sup> The change in  $\nu_B$  measured on heating became sharper at about 137 °C compared to the relatively broad minimum obtained upon cooling. This is accompanied by much larger  $\Gamma_B$  recorded upon heating than

upon cooling. This thermal hysteresis may be related to the evolution of PNRs and polar domains in the low-temperature phase. This kind of aging phenomena has often been observed from nonequilibrium state in disordered systems like relaxor, dipolar glasses, spin glasses, etc.

Figure 1(b) shows the Brillouin spectra of the same crystal before and after poling (denoted as “unpoled” and “poled”, respectively, in the figure) at 30 °C. The application of dc bias field of 15 kV/cm induces several interesting changes in the Brillouin spectrum: (1) hardening of the LA mode frequency and decrease in its half width, (2) suppression of the CP intensity, and (3) the appearance of the TA mode. Since the electric field of 15 kV/cm is lower than the coercive field required to induce the tetragonal symmetry,<sup>19</sup> the [001]<sub>c</sub>-poled PIN-PMN-PT is expected to have a multi-domain (or domain-engineered) state composed of four  $\langle 111 \rangle$  rhombohedral domains<sup>1</sup> and may be considered to have a tetragonal symmetry on average. In this case, the observed LA and TA modes may correspond to the  $C_{33}$  and  $C_{44}$  elastic constants, respectively. The discontinuous change in the LA mode frequency and the appearance of the TA mode reflects the transformation from the relaxor-like state (or slightly distorted mesoscopic ferroelectric state) into a domain-engineered state.<sup>1</sup> In addition, the fact that the TA mode persists when the dc bias field is turned off indicates that the field-induced structural change remains stable even without the dc bias field. Room-temperature Brillouin frequency shifts were obtained from the measured spectrum to calculate the elastic constants of poled sample and to compare them with previous reports. When the reported density of 8102 kg/cm<sup>3</sup> and the average refractive index 2.66 (at the wavelength of 546 nm) of PMN-35%PT are considered,<sup>11,26</sup> the elastic constants  $C_{33}$  and  $C_{44}$  of the poled sample are calculated to be 16.5 and 6.65 GPa at room temperature. These numerical values are very similar to the reported elastic constants ( $C_{33}^D = 16.7$  and  $C_{44}^D = 7.0$  GPa) of the [001]<sub>c</sub>-poled PIN-PMN-PT single crystal of a similar composition obtained in terms of the resonance method.<sup>8</sup> This result seems to suggest that acoustic dispersion effect between the resonance technique and hypersonic Brillouin scattering might be very small in PIN-PMN-PT of this composition.

Figure 3 shows the Brillouin shift of the LA mode along with the dielectric data of the poled sample as a function of temperature measured upon heating. The dielectric permittivity shows two clear anomalies at  $\sim 116$  ° and  $\sim 165$  °C consistent with dielectric properties of previous study carried out on similar compositions.<sup>19</sup> In addition, these two dielectric anomalies are correlated with the step-like changes in the elastic property. The fact that the high-temperature anomalies of both measurements do not appear at exactly the same temperature is not surprising because the dielectric anomaly has some frequency dispersion and the dielectric maximum temperature depends on the probe frequency. The comparisons of the temperature dependence of  $\nu_B$  and  $\Gamma_B$  of unpoled and poled samples are shown in Figs. 4(a) and 4(b), respectively, obtained at the heating process. The two insets (c) and (d) of Fig. 4 show the extended plot of  $\nu_B$  of the LA mode and the intensity changes of both modes, respectively, of the poled sample near the ferroelectric phase transitions.

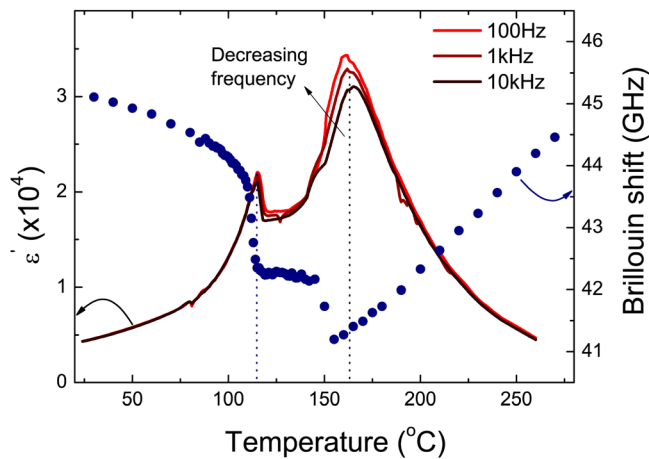


FIG. 3. (Color online) The temperature dependence of the dielectric permittivity and the Brillouin shift of the poled PIN-PMN-PT single crystal.

The temperature dependence of  $\nu_B$  and  $\Gamma_B$  clearly shows that the two step-like changes in  $\nu_B$  are correlated to the hyper-sonic damping peaks at almost the same temperatures. The inset (d) of Fig. 4 shows that the TA mode intensity becomes zero at  $\sim 116^\circ\text{C}$ , which is a clear evidence for a structural phase transition at this temperature. Based on the observed transition temperatures and comparison with previous stud-

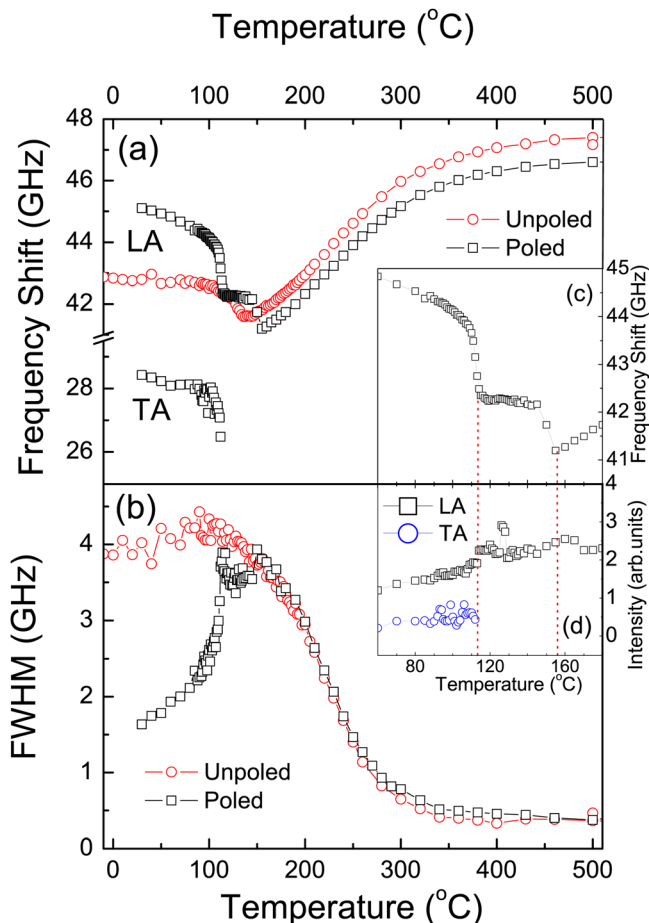


FIG. 4. (Color online) The temperature dependences of (a) the Brillouin frequency shift and (b) the FWHM of the LA and TA modes of both the unpoled and poled samples measured on heating process. The insets (c) and (d) show the extended plot of  $\nu_B$  and the mode intensities of the poled sample near the ferroelectric phase transitions, respectively.

ies,<sup>19</sup> we attribute the observed two dielectric and elastic anomalies to the successive phase transitions from rhombohedral to tetragonal and then from tetragonal to cubic phases with increasing temperature.

We note that the high-temperature tetragonal-cubic phase transition remains somewhat diffused characterized by the frequency dispersion and a smeared change in  $\nu_B$  compared to PMN-*x*PT.<sup>24</sup> The diffuseness of the dielectric property at the Curie temperature has also been observed from other PIN-PMN-PT single crystals,<sup>8,19</sup> which is in contrast to the sharp, discontinuous changes in the dielectric and elastic properties of PZN-*x*PT and PMN-*x*PT near MPB at the cubic-tetragonal phase transition temperature. This may be understood based on the suggestion by Chen *et al.* of an intermediate state below the dielectric maximum temperature on approaching the cubic phase.<sup>20</sup> They reported that [001]-oriented 0.34PIN-0.25PPM-0.41PT exhibited an intermediate state via which transformation from macrodomain to microdomain states occurs. The macroscopic long-range polar order formed under high dc bias field does not disappear abruptly at the phase transition but changes into microdomains due to inherent disorder and random fields in relaxors. Finally, we point out that the temperature range of the intermediate tetragonal phase may be changed and controlled depending on the previous poling treatment. When the crystal was poled under the same electric field at  $-30^\circ\text{C}$  and the Brillouin spectrum was measured upon heating without the dc bias field, the temperature dependence of  $\nu_B$  and  $\Gamma_B$  showed two clear anomalies at  $\sim 100^\circ$  and  $\sim 125^\circ\text{C}$ . This means that the intermediate temperature range can be reduced significantly by using poling at lower temperatures.

#### IV. CONCLUSION

In conclusion, we compared the phase transition behaviors of unpoled and [001]<sub>c</sub>-poled PIN-PMN-PT single crystals by using Brillouin light scattering and dielectric spectroscopies. The unpoled sample showed broad elastic softening along with substantial dielectric dispersion, which are typical in relaxors. The Burns temperature was determined to be about  $320^\circ\text{C}$  by observing the spectral changes in central peaks and the corresponding change in the relaxation time. The small damping peak at  $\sim 90^\circ\text{C}$  was attributed to the development of moderately diffused and short-ranged (or mesoscopic) polar state due to the abrupt growth and merging of polar nanoregions without changing the directions of their dipole moments. Poling the crystal under DC bias field of 15 kV/cm along the [001]<sub>c</sub> direction gave rise to the appearance of the TA mode, suppression of the central peak, and substantial changes in the LA mode properties, indicating structural transformation from the short-range polar state into a domain-engineered rhombohedral state. The temperature dependence of dielectric and elastic properties of the poled sample exhibited two clear anomalies at  $\sim 116^\circ$  and  $\sim 165^\circ\text{C}$ . These two-step changes were attributed to the successive phase transitions from rhombohedral to tetragonal and then from tetragonal to cubic phases with increasing temperature based on the observed transition temperatures and comparison with previous studies. The high-temperature

tetragonal-cubic phase transition remained diffused even for the poled sample, which may be understood as the transformation of macrodomains into microdomains upon heating due to local random fields inherent in relaxors.

## ACKNOWLEDGMENTS

One of authors (SK) are thankful to TRS technologies, Inc. for providing [001] oriented PIN-PMN-PT crystal plates. J.-H. Ko is thankful to the JSPS short-term Fellowship Program for his stay at the University of Tsukuba in 2011. This research was supported in part by Basic Science Research Program through the National Research Foundation of Korea (NRF) funded by the Ministry of Education, Science and Technology (2010-0010497).

<sup>1</sup>S.-E. Park and T. R. Shrout, *J. Appl. Phys.* **82**, 1804 (1997).

<sup>2</sup>*Handbook of Advanced Dielectric, Piezoelectric, and Ferroelectric Materials Synthesis, Properties and Applications*, edited by Z. G. Ye (Woodhead, Cambridge, 2008).

<sup>3</sup>F. Li, S. Zhang, Z. Xu, X. Wei, and T. R. Shrout, *Adv. Funct. Mater.* **21**, 2118 (2011).

<sup>4</sup>Y. Hosono, Y. Yamashita, K. Hirayama, and N. Ichinose, *Jpn. J. Appl. Phys.* **44**, 7037 (2005).

<sup>5</sup>G. Xu, K. Chen, D. Yang, and J. Li, *Appl. Phys. Lett.* **90**, 032901 (2007).

<sup>6</sup>J. Tian, P. Han, X. Huang, H. Pan, J. F. Carroll III, and D. A. Payne, *Appl. Phys. Lett.* **91**, 222903 (2007).

<sup>7</sup>P. Yu, F. Wang, D. Zhou, W. Ge, X. Zhao, H. Luo, J. Sun, X. Meng, and J. Chu, *Appl. Phys. Lett.* **92**, 252907 (2008).

<sup>8</sup>S. Zhang, J. Luo, W. Hackenberger, and T. R. Shrout, *J. Appl. Phys.* **104**, 064106 (2008).

<sup>9</sup>S. Zhang, J. Luo, W. Hackenberger, N. P. Sherlock, R. J. Meyer, Jr., and T. R. Shrout, *J. Appl. Phys.* **105**, 104506 (2009).

<sup>10</sup>X. Liu, S. Zhang, J. Luo, T. R. Shrout, and W. Cao, *J. Appl. Phys.* **106**, 074112 (2009).

<sup>11</sup>X. Liu, S. Zhang, J. Luo, T. R. Shrout, and W. Cao, *Appl. Phys. Lett.* **96**, 012907 (2010).

<sup>12</sup>E. Sun, S. Zhang, J. Luo, T. R. Shrout, and W. Cao, *Appl. Phys. Lett.* **97**, 032902 (2010).

<sup>13</sup>P. Finkel, H. Robinson, J. Stace, and A. Amin, *Appl. Phys. Lett.* **97**, 122903 (2010).

<sup>14</sup>S. Zhang, F. Li, J. Luo, R. Xia, W. Hackenberger, and T. R. Shrout, *Appl. Phys. Lett.* **97**, 132903 (2010).

<sup>15</sup>F. Li, S. Zhang, Z. Xu, X. Wei, J. Luo, and T. R. Shrout, *J. Appl. Phys.* **107**, 054107 (2010).

<sup>16</sup>W. Wang, D. Liu, Q. Zhang, B. Ren, Y. Zhang, J. Jiao, D. Lin, X. Zhao, and H. Luo, *J. Appl. Phys.* **107**, 084101 (2010).

<sup>17</sup>Q. Li, Y. Liu, J. Schiemer, P. Smith, Z. Li, R. L. Withers, and Z. Xu, *Appl. Phys. Lett.* **98**, 092908 (2011).

<sup>18</sup>P. Finkel, K. Benjamin, and A. Amin, *Appl. Phys. Lett.* **98**, 192902 (2011).

<sup>19</sup>F. Li, S. Zhang, D. Lin, J. Luo, Z. Xu, X. Wei, and T. R. Shrout, *J. Appl. Phys.* **109**, 014108 (2011).

<sup>20</sup>Y. Chen, K. H. Lam, D. Zhou, X. S. Gao, J. Y. Dai, H. S. Luo, and H. L. W. Chan, *J. Appl. Phys.* **109**, 014111 (2011).

<sup>21</sup>S. Zhang, G. Liu, W. Jiang, J. Luo, W. Cao, and T. R. Shrout, *J. Appl. Phys.* **110**, 064108 (2011).

<sup>22</sup>R. Vacher, and L. Boyer, *Phys. Rev. B* **6**, 639 (1972).

<sup>23</sup>For a review, A. A. Bokov and Z.-G. Ye, *J. Mater. Sci.* **41**, 313 (2006).

<sup>24</sup>J.-H. Ko, D. H. Kim, S. Tsukada, S. Kojima, A. A. Bokov, and Z.-G. Ye, *Phys. Rev. B* **82**, 104110 (2010).

<sup>25</sup>J.-H. Ko, D. H. Kim, S. Kojima, W. Chen, and Z.-G. Ye, *J. Appl. Phys.* **100**, 066106 (2006).

<sup>26</sup>C. He, F. Wang, D. Zhou, X. Zhao, D. Lin, H. Xu, T. He, and H. Luo, *J. Phys. D: Appl. Phys.* **39**, 4337 (2006).